NeuroImage 236 (2021) 118072

Contents lists available at ScienceDirect

NeuroImage

journal homepage: www.elsevier.com/locate/neuroimage

Brain state-based detection of attentional fluctuations and their modulation

Ayumu Yamashita[a,b,c,*], David Rothlein[a,b,f], Aaron Kucyi[d], Eve M. Valera[e,g], Michael Esterman[a,b,f]

[a] Boston Attention and Learning Laboratory, VA Boston Healthcare System, Massachusetts,02130. United States
[b] Department of Psychiatry, Boston University School of Medicine, Massachusetts, 02118. United States
[c] Overseas Research Fellow, Japan Society for the Promotion of Science, Tokyo,102-0083. Japan
[d] Department of Psychology, Northeastern University, Massachusetts, 02115. United States
[e] Department of Psychiatry, Harvard Medical School, Massachusetts, 02215. United States
[f] National Center for PTSD, VA Boston Healthcare System, Massachusetts, 02130. United States
[g] Department of Psychiatry, Massachusetts General Hospital, Massachusetts, 02125, United States

ARTICLE INFO

Keywords:
Sustained attention
fMRI
Energy landscape
Motivation
Mind wandering
ADHD

ABSTRACT

In the search for brain markers of optimal attentional focus, the mainstream approach has been to first define attentional states based on behavioral performance, and to subsequently investigate "neural correlates" associated with these performance variations. However, this approach constrains the range of contexts in which attentional states can be operationalized by relying on overt behavior, and assumes a one-to-one correspondence between behavior and brain state. Here, we reversed the logic of these previous studies and sought to identify behaviorally-relevant brain states based solely on brain activity, agnostic to behavioral performance. In four independent datasets, we found that the same two brain states were dominant during a sustained attention task. One state was behaviorally optimal, with higher accuracy and stability, but a greater tendency to mind wander (State1). The second state was behaviorally suboptimal, with lower accuracy and instability (State2). We further demonstrate how these brain states were impacted by motivation and attention-deficit/hyperactivity disorder (ADHD). Individuals with ADHD spent more time in suboptimal State2 and less time in optimal State1 than healthy controls. Motivation overcame the suboptimal behavior associated with State2. Our study provides compelling evidence for the existence of two attentional states from the sole viewpoint of brain activity.

1. Introduction

Attention is not constant but fluctuates from moment to moment between optimal and suboptimal focus (Esterman and Rothlein, 2019; Fiebelkorn and Kastner, 2019; Fiebelkorn et al., 2018; Helfrich et al., 2018; Mackworth, 1948). The elucidation of the brain mechanisms required to sustain optimal attention is theoretically important and translationally relevant (Chun et al., 2011; Fortenbaugh et al., 2017a; Fortenbaugh et al., 2017b; Fortenbaugh et al., 2018; Huang-Pollock et al., 2012; Marchetta et al., 2008; Rosenberg et al., 2017; Rosenberg et al., 2016a). To understand the neural substrate of sustained attention, two mainstream approaches have been taken. The first has been to examine differences in brain activity based on attention fluctuations in behavioral performance (behavior to brain activity). The second approach has been to investigate the relationship between the brain connectome and sustained attention ability (behavior to connectome). Each of these approaches has advanced our understanding of sustained attention, but nonetheless has limitations.

Using the first approach, a wealth of previous studies dichotomized attention fluctuations into optimal and suboptimal states based on behavioral performance (stable reaction times or fewer attentional lapses/errors, less mind wandering, and vice versa) and investigated the differences in brain activity between these behaviorally inferred attentional states (Drummond et al., 2005; Esterman et al., 2013; Fortenbaugh et al., 2017b; Fortenbaugh et al., 2018; Hilti et al., 2013; Hinds et al., 2013; Kelly et al., 2008; Kessler et al., 2016; Kucyi et al., 2017; Langner and Eickhoff, 2013; Lawrence et al., 2003; Weissman et al., 2006). Almost all studies have reported contrasting brain-behavior relationships with brain regions in the default mode network (DMN), dorsal attention network (DAN) and salience network (SAN), which are major intrinsic brain networks (Laird et al., 2011). In a growing number of studies, optimal performance states were associated with greater DMN activity, while suboptimal performance states were associated with greater DAN and SAN activity (Esterman et al., 2013; Fortenbaugh et al., 2018; Kucyi et al., 2016; Kucyi et al., 2017). However, such approaches, which infer mental states based on behavior, implicitly assume a one-to-one correspondence between behavior and brain state. This constrains the estimated brain state. For example, suboptimal attention (periods of low accuracy) could result from multi-

* Corresponding author.
E-mail addresses: ayamashi@bu.edu, ayumu@atr.jp (A. Yamashita).

https://doi.org/10.1016/j.neuroimage.2021.118072.
Received 26 September 2020; Received in revised form 30 March 2021; Accepted 9 April 2021
Available online 18 April 2021.

ple distinct causes, such as hyper- or hypo-arousal, external distraction, or mind wandering (Esterman and Rothlein, 2019). These could be reflected in distinct brain states, albeit with similar behavior (e.g., lower accuracy). Such brain states could not be detected by relying on accuracy alone. Furthermore, these approaches rely on frequent responses from participants, which constrains the types of tasks that can be used to identify attentional states.

In addition to relating behavioral differences to brain activity, previous studies have shown relationships between individual differences in sustained attention ability and the brain's functional connectome, defined as pairwise temporal correlations between brain regions (Fortenbaugh et al., 2018; Kelly et al., 2008; Rosenberg et al., 2017; Rosenberg et al., 2016a; Thompson et al., 2013). For example, participants who have stronger anticorrelation between DMN and DAN/SAN tend to perform better (Fortenbaugh et al., 2018; Kelly et al., 2008; Kucyi et al., 2020; Thompson et al., 2013), and connectivity patterns outside of these networks can also predict individual differences in sustained attention performance (Rosenberg et al., 2016a; Rosenberg et al., 2020). These findings implicate connectivity within and between functionally different intrinsic brain networks in supporting sustained attention ability across individuals. Recent work has also shown that within-subject attentional fluctuations vary with DAN-DMN connectivity as well as multivoxel information processing-based measures (Rothlein et al., 2018). Nonetheless, whether and how the connectome across different intrinsic brain networks supports sustained attention performance via the intermediary of brain activity patterns remains unclear.

To address these limitations in the link between brain activity and attentional states, we estimated brain states on the sole basis of brain activity during a sustained attention task, and examined if these brain states had reliable and replicable differences in task performance. Although there are several methods for estimating brain state from brain activity alone, such as Gaussian mixture modeling and hidden Markov models (Ezaki et al., 2020), we used an energy landscape approach which describes a brain state as a brain activity pattern based on the brain's connectome (Ezaki et al., 2018; Ezaki et al., 2017; Watanabe et al., 2014a; Watanabe et al., 2014b; Watanabe and Rees, 2017). The motivation for the use of the energy landscape analysis was that previous studies have shown that brain activity during multi-stable behaviors can be described as a series of brain states and transitions between different attractors on the energy landscape (Deco et al., 2009; Friston et al., 2012; Watanabe et al., 2014b), and such attractors are constrained by the brain's connectome (Deco et al., 2012). In other words, the strength of connectivity across brain regions determines the stable brain states (attractors), which are represented as brain activity patterns. Therefore, we hypothesized that sustained attention fluctuates in concert with brain activity patterns across intrinsic brain networks on the energy landscape (brain states), thereby bridging the inter-relationships between behavior, connectome, and brain activity pattern. In particular, we sought to examine the relationship between attentional state and brain-state using this brain-first approach by asking two broad questions: (1) can stable brain states be identified during a sustained attention task and if so, how many?, (2) do the identified stable brain states correspond to consistent differences in task performance?

In addition to examining objective performance differences between brain states during sustained attention, we replicated and extended these analyses to consider other factors that impact sustained attention. Specifically, suboptimal sustained attention is commonly associated with self-reported mind wandering (Christoff et al., 2009; Kucyi et al., 2016; Mittner et al., 2016). Therefore, using a dataset with intermittent thought probes, we investigated not only differences in behavioral performance but also differences in self-reported mind-wandering between brain states. Additionally, it is frequently observed that individuals with neuropsychiatric disorders of attention such as attention-deficit hyperactivity disorder (ADHD) have impaired sustained attention performance compared to healthy controls (Castellanos et al., 2006; Castellanos and Tannock, 2002; Fortenbaugh et al., 2017b; Hauser et al., 2016; Huang-Pollock et al., 2012; Marchetta et al., 2008; Rosenberg et al., 2016a). On the other hand, it is known that extrinsic motivation improves sustained attention performance (Esterman et al., 2017a; Esterman et al., 2014a; Reteig et al., 2019). Using an fMRI dataset of individuals with ADHD, and another dataset that manipulated motivation, we examined four possible ways these conditions could impact the observed brain states as follows: (1) the factor directly impacts the nature of the brain state(s) (alters the brain activity pattern of the brain state), (2) the factor impacts the dwell time in the brain state(s) (3) the factor impacts performance across all brain states equally, (4) the factor impacts performance differentially in a subset of brain states. Together, we examined four datasets to discover and replicate the existence of behaviorally relevant brain states, described as activity patterns across the brain's networks. Furthermore, by using intermittent thought-probes we measured self-reported mind-wandering and compared the degree of mind wandering between brain states. Finally, we considered how ADHD and motivation impacts the characteristics of these brain states.

2. Materials and methods

2.1. Overview of analyses

We first demonstrated and validated a novel approach for defining brain states based on brain activity during a sustained attention task agnostic to behavioral performance, and compared behavioral performance between brain states. Next, we investigated whether these states and behavioral differences could be replicated with three independent datasets. Furthermore, by using intermittent thought-probes, we measured self-reported mind-wandering and compared the degree of mind wandering between brain states. Finally, we demonstrated the influence of ADHD and motivation on these states.

We measured brain activity using functional magnetic resonance imaging (fMRI) during a gradual onset continuous performance task (gradCPT). The gradCPT is a well-validated test of sustained attention, previously used to define attentional states based on reaction time variability fluctuations over time (Esterman et al., 2013; Fortenbaugh et al., 2015; Fortenbaugh et al., 2018). In order to estimate brain states, we used a novel energy landscape analysis. Since attractors in the energy landscape are local minima in brain activity patterns, a brain activity pattern can be defined as a brain state in a manner that is agnostic to behavior. Using Dataset 1, we thus examined the observed number of brain states during sustained attention, and whether performance differed during these distinct brain states. To statistically investigate the difference in behavioral performance between brain states, we conducted two-tailed *t*-tests and calculated Hedges's *g* as the effect size (Bonett, 2009; Hedges, 1981). We did not control for multiple comparisons for this analysis, because we confirmed its reproducibility by performing the same analysis on all 4 independent datasets. Next, we provided additional support for these results using an independent validation dataset for replication by using Dataset 2. Furthermore, with Dataset 2, by using intermittent thought-probes we measured self-reported mind-wandering and compared the degree of mind wandering between brain states. To further replicate and extend these results, we based an additional set of experiments on studies that have shown that sustained attention is improved by motivation (Esterman et al., 2017a; Esterman et al., 2014a; Reteig et al., 2019) and impaired in individuals with ADHD (Fortenbaugh et al., 2017b; Huang-Pollock et al., 2012; Marchetta et al., 2008; Rosenberg et al., 2017; Rosenberg et al., 2016a).

Table 1
Imaging protocols in every dataset.

Dataset	Dataset 1	Dataset 2	Dataset 3	Dataset 4
Number of participants	16	29	19	16
MRI scanner	MAGNETOM Trio	CONNECTOM	CONNECTOM	MAGNETOM Trio
Magnetic field strength	3T	3T	3T	3T
Channels per coil	12	64	64	32
Scan parameters for functional image				
Field of view (mm)	192 × 192	110 × 110	110 × 110	192 × 192
Matrix	64 × 64	55 × 55	55 × 55	64 × 64
Number of slices	33	68	68	33
Number of volumes	248 for gradCPT 188 for rsfMRI	*About 490	*About 490	248
Slice thickness (mm)	3	2	2	3
TR (ms)	2,000	1,080	1,080	2,000
TE (ms)	30	30	30	30
Total scan time (min: s)	8:16 for gradCPT 6:16 for rsfMRI	*About 8:48	*About 8:48	8:16
Flip angle (degree)	90	60	60	90
Gradual onset continuous performance task (gradCPT)				
Task type	Original gradCPT	gradCPT with thought probe	gradCPT with thought probe	gradCPT with reward
Inter stimulus interval (ms)	800	1,300	1,300	800
Number of runs	3	4	4	3–5
Scan parameters for structural image				
TR (ms)	2,530	2,530	2,530	2,530
TE (ms)	3.32	1.15	1.15	3.32
Flip angle (degree)	7°	7°	7°	7°
Field of view (mm)	256 × 256	256 × 256	256 × 256	256 × 256
In-plane resolution (mm^2)	1.0	1.0	1.0	1.0
Slice thickness (mm)	1.0	1.0	1.0	1.0

* The number of volumes in Dataset 2 were different across subjects and runs, the mean number of volumes collected per run averaged 490.

Specifically, we used Dataset 3, a gradCPT dataset in adults with ADHD, and Dataset 4, a gradCPT dataset with and without reward-based motivation to investigate how ADHD and motivation impact the brain states and behavioral performance during these states. For our statistical analyses, we applied mixed-effects linear regression models to the dwell time and behavioral performance with brain state, the additional factors (motivation, ADHD), and their interaction as fixed effects, and subject as a random effect. We tested the fixed effects with *t*-tests on mixed effects model. We calculated Cohen's f^2 for fixed effects as the effect size (Lorah, 2018) . In these analyses with the additional factors, we report *p*-values with and without correction for multiple comparisons. Corrections for multiple testing were performed with the false discovery rate (FDR) procedure (Benjamini and Hochberg, 1995; Benjamini and Yekutieli, 2001, 2005) for the number of hypotheses (4 measurements for motivation and 5 measurements for ADHD). In the following sections, we first explain the gradCPT task and fMRI analyses that are common to all datasets, followed by dataset-specific details.

2.2. gradual onset continuous performance task

The gradCPT contained 10 round, grayscale photographs of mountain scenes and 10 of city scenes. These scenes were randomly presented with 10% mountain and 90% city, without allowing the identical scene to repeat on consecutive trials. Scene images gradually transitioned from one to the next, using a linear pixel-by-pixel interpolation, with each transition occurring in 800 ms (fast version; Dataset 1 and Dataset 2) or 1300 ms (slow version; Dataset 3 and Dataset 4) (Table 1). Participants were instructed to press a button for each city scene, and withhold responses to mountain scenes. Response accuracy was emphasized without reference to speed. However, given that the next stimulus would replace the current stimulus in 800/1300 ms, a response deadline was implicit in the task.

2.2.1. Calculation of reaction time

Reaction times (RT) were calculated relative to the beginning of each image transition, such that an RT of 800/1300 ms (slow vs. fast versions, see Table 1) indicates a button press at the moment image n was 100% coherent and not mixed with other images. A shorter RT indicates that the current scene was still in the process of transitioning from the previous, and a longer RT indicates that the current scene was in the process of transitioning to the subsequent scene. So, for example, an RT of 720/1170 ms would be at the moment of 90% image n and 10% image n − 1, and so forth. On rare trials with highly deviant RTs (before 70% coherence of image n and after 40% coherence of image n + 1) or multiple button presses, an iterative algorithm maximized correct responses as follows. The algorithm first assigned unambiguous correct responses, leaving few ambiguous button presses (presses before 70% coherence of the current scene and after 40% coherence of the following scene or multiple presses occurred on < 5% of trials). Second, ambiguous presses were assigned to an adjacent trial if 1 of the 2 had no response. If both adjacent trials had no response, the press was assigned to the closest trial, unless one was a no-go target, in which case subjects were given the benefit of the doubt that they correctly omitted. Finally, if there were multiple presses that could be assigned to any 1 trial, the fastest response was selected. Slight variations to this algorithm yielded highly similar results, as most button presses showed a 1–1 correspondence with presented images (Esterman et al., 2013).

2.2.2. Calculation of reaction time variability

Although attentional fluctuations are commonly assessed with accuracy measures, another way in which subtler trial-to-trial variations have been explored is through the analysis of RT variability (Esterman et al., 2013; MacDonald et al., 2009; MacDonald et al., 2006). High RT variability has been specifically linked to impairments of attention and executive function in individuals with ADHD (Castellanos et al.,

2006). RT variability was computed from the correct responses in each run (following z-transformation of RTs within-subject to normalize the scale of the RT variability), where the value assigned to each trial represented the absolute deviation of the trial's RT from the mean RT of the run. We reasoned that deviant RTs, whether fast or slow, represented reduced attention to the task as follows: extremely fast RTs often indicate premature responding and inattention to the potential need for response inhibition (Cheyne et al., 2009), while extremely slow RTs might indicate reduced attention to or inefficient processing of the ongoing stream of visual stimuli, requiring more time to accurately discriminate scenes (Weissman et al., 2006). Values for trials without responses (omission errors and correct trials) were interpolated linearly, such that the missing values were linearly estimated from RTs of the 2 surrounding trials. A smoothed RT variability time course was computed using a Gaussian kernel of 9 trials (~7 s) full-width at half-maximum (FWHM), thus integrating information from the surrounding 20 trials, or 16 s, via a weighted average. This choice was based on prior work linking fluctuations around this frequency to attentional impairments (Di Martino et al., 2008).

2.2.3. Calculation of accuracy

In addition to mean RT and RT variability, we calculated performance accuracy (d prime). d prime is an index of accuracy, or perceptual sensitivity, that can simultaneously account for hit rate and false alarm rate. In this case, a hit indicates correct omission to the mountain image (correct omission), and a false alarm is a failure to response to a city scene (omission error); d prime was calculated as z(hit rate) − z(false alarm rate). Here z is normal probability density function in SciPy (Virtanen et al., 2019).

2.3. fMRI analysis

Imaging protocols are summarized in Table 1 for all datasets.

2.3.1. Preprocessing

We performed preprocessing of the fMRI data using FMRIPREP version 1.3.0 (Esteban et al., 2019). Preprocessing steps included realignment, coregistration, segmentation of T1-weighted structural images, normalization to Montreal Neurological Institute space. For more details of the pipeline, see http://fmriprep.readthedocs.io/en/latest/workflows.html.

2.3.2. fMRI signal extraction from brain networks

We extracted the time series of blood oxygen level dependent (BOLD) from each of 400 regions of interest (ROIs). The 400 ROIs were defined as 4-mm spheres around the center coordinates that were determined in the previous studies (Schaefer et al., 2018) (Fig. 1a). The BOLD signal time courses were extracted with spatial smoothing using an isotropic Gaussian kernel of 6 mm full-width at half-maximum from these 400 ROIs.

To remove several sources of spurious variance from the 400 ROIs' signal time courses, we used linear regression with eighteen regression parameters, including six motion parameters, an average signal over the whole brain, six physiological noise regressors, and five event-related task regressors on the BOLD response time course. Six physiological noise regressors were extracted by applying CompCor (Behzadi et al., 2007). Principal components were estimated for the anatomical CompCor (aCompCor). A mask to exclude signals with a cortical origin was obtained by eroding the brain mask and ensuring that it contained subcortical structures only. Six aCompCor components were calculated within the intersection of the subcortical mask and union of the CSF and WM masks calculated in T1-weighted image space after their projection to the native space of functional images in each session. To account for and regress out task events (commission error, correct omission, correct commission, omission error) and trial-to-trial RT, we estimated BOLD response time courses of each event type by using *hemodynamic_models* function implemented in Nistat (https://nistats.github.io/). To account for variance and mean differences across run and participant, we standardized the BOLD signal time course for each ROI (shifted to zero mean and scaled to unit variance) after noise regression. These ROIs were then classified into seven functionally different brain networks (Schaefer et al., 2018) (Fig. 1a). For each participant, we then calculated seven time series that represented the activity of these brain networks (Fig. 1b) by averaging BOLD signal time courses in the 400 ROIs corresponding to those brain networks. Using the voxel-wise network average time series instead of the ROI-wise network average produced nearly identical patterns of results.

2.3.3. Pairwise maximum entropy model

We fit the pairwise Maximum entropy model (MEM) to the preprocessed BOLD signals as follows in the same manner as that employed in previous studies (Ezaki et al., 2018; Ezaki et al., 2017; Watanabe et al., 2013, 2014a; Watanabe et al., 2014b; Watanabe and Rees, 2017). We used open toolbox so called Energy Landscape Analysis Toolkit (https://sites.google.com/site/ezakitakahiro/software). For each network activity time series, we first binarized the obtained BOLD signals with a threshold that was defined as the time-averaged activity of the network activity. We then concatenated BOLD signals from all runs and all participants for each network activity. Previous studies suggest that binarization does not eliminate important information contained in originally continuous brain signals (Watanabe et al., 2013, 2014a; Watanabe et al., 2014b). In this method, the binarized activity σ_i^t at network i and discrete time t is either active or inactive (+1 or 0). The activity pattern at time t is described by $V^t = [\sigma_1^t, \sigma_2^t, \ldots, \sigma_N^t]^{\mathrm{T}}$ where N (=7) is the number of the networks. The kth brain activity pattern is described by V_k ($k = 1, 2, \ldots, 2^N$). Especially, when the empirical activation of network i, $\langle \sigma_i \rangle = (1/T) \sum_{t=1}^{T} \sigma_i^t$, and the empirical pairwise interaction between networks i and j, $\langle \sigma_i \sigma_j \rangle = (1/T) \sum_{t=1}^{T} \sigma_i^t \sigma_j^t$, where T is the number of volumes, are estimated from the data, the probability distribution of the kth brain activity pattern with the largest entropy is the Boltzmann distribution (Jaynes, 1957). That is, $P(V_k) = e^{E(V_k)} / \sum_{l=1}^{2^N} e^{-E(V_l)}$, where $E(V_k)$ is the energy of activity pattern V_k and is given by

$$E(V_k) = -\sum_{i=1}^{N} h_i \sigma_i(V_k) - \frac{1}{2} \sum_{i=1}^{N} \sum_{j=1,\ j \neq i}^{N} J_{ij} \sigma_i(V_k) \sigma_j(V_k). \quad (1)$$

Here, $\sigma_i(V_k)$ represents the binarized activity (+1 or 0) at region i under activity pattern V_k. We calculated h_i and J_{ij} by maximum likelihood estimation to adjust the model-based activation of network i, $\langle \sigma_i \rangle_{model}$ and the model-based pairwise interaction between networks i and j, $\langle \sigma_i \sigma_j \rangle_{model}$ toward the empirical activation of network i, $\langle \sigma_i \rangle$ and the empirical pairwise interaction between networks i and j, $\langle \sigma_i \sigma_j \rangle$, respectively. Here, $\langle \sigma_i \rangle_{model} = \sum_{l=1}^{2^N} \sigma_i(V_l) P(V_l)$ and $\langle \sigma_i \sigma_j \rangle_{model} = \sum_{l=1}^{2^N} \sigma_i(V_l) \sigma_j(V_l) P(V_l)$. Please note that this energy value does not indicate any biological energy. It is rather a statistical index that indicates the occurrence probability of each brain activity pattern. For instance, activity patterns with lower energy values tend to occur more frequently. Of note, in equation (1) the energy of activity pattern V_k depends on J_{ij}, which is known to represent the anatomical connection between networks i and j (Watanabe et al., 2013). That is, the energy of activity pattern V_k is based on the connectome across networks.

We confirmed whether the pairwise MEM accurately fit to the data by calculating Pearson's correlation coefficient between empirical appearance probability and model appearance probability $P(V_k)$ (Supplementary Figure 1). Empirical appearance probability of brain activity

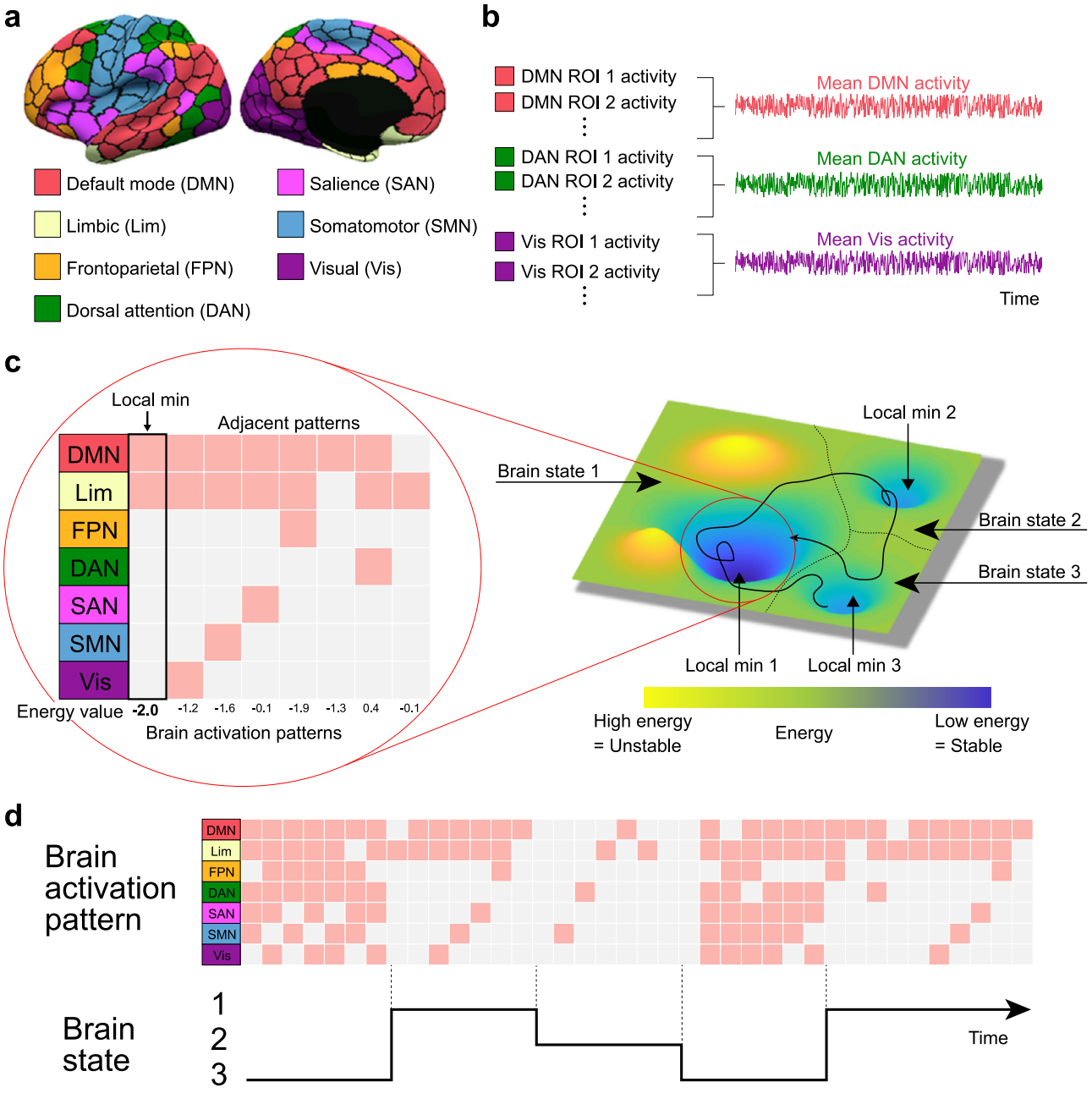

Fig. 1. Procedures of energy landscape analysis. (a) Region of interests (ROIs) from Schaefer atlas (Schaefer et al., 2018). The color indicates functionally different brain networks. (b) Blood oxygen level dependent (BOLD) signals of seven functionally different brain networks were calculated as average BOLD signals in the 400 ROIs corresponding to those brain networks. (c) Hypothetical energy landscape and local minima brain activity pattern and adjacent patterns. Individual brain activity patterns are represented as each brain region being active (pink) or inactive (white). (d) Hypothetical time course of brain activation patterns to time course of brain state. DMN: default mode network; Lim: limbic; FPN: frontoparietal network; DAN: dorsal attention network; SAN: salience network; SMN: somatomotor network; Vis: visual.

pattern V_k is calculated by $(1/T)\sum_{t=1}^{T} z_k^t$, where $\mathbf{z}^t$ is a K-dimensional binary variable having a 1-of-K representation in which a particular element z_k^t is equal to 1 and all other elements are equal to 0. The values of z_k^t therefore satisfy $z_k^t \in \{0,1\}$ and $\sum_k z_k^t = 1$, and we see that there are K $(=2^N)$ possible brain activity patterns for the vector $\mathbf{z}^t$ at time t according to which element is nonzero. In non-technical terms, this confirms whether the model successfully fit the data.

2.3.4. Energy landscape analysis (Definition of brain state)

We calculated the energy landscape as done in the previous studies (Ezaki et al., 2018; Ezaki et al., 2017; Watanabe et al., 2014b; Watanabe and Rees, 2017). The energy landscape is defined as a graph of brain activity patterns V_k with the corresponding energy $E(V_k)$. Two activity patterns are regarded as adjacent in the graph if they take the opposite binary activity at just one brain region. We first exhaustively searched for local energy minima, whose energy value is smaller than those of all the N adjacent patterns (Fig. 1c). We then summarized all brain activity patterns into local minimum brain states. The number of

brain states (local minimum brain states) is determined in a data-driven manner. We first selected a starting brain activity pattern i among the 2^N brain activity patterns. Then, if any of its neighbor patterns has a smaller value of energy than pattern i, we moved to the neighbor pattern with the smallest energy value. Otherwise, we did not move, which implied that pattern i was a local minimum. We repeated this procedure until arriving at a local minimum. The starting pattern i was regarded to belong to the local minimum brain state that was finally reached. We estimated the corresponding local minimum brain state for all brain activity patterns, so that we could estimate the time series of brain states from the time series of brain activity patterns (Fig. 1d).

2.3.5. Calculation of dwell time in a brain state

A percentage of dwell time in each brain state $S_{k'}$ is calculated by $100 \times (1/T') \sum_{t=1}^{T'} s_{k'}^t$ for each participant, where T' is the number of volumes in each participant and $s_{k'}^t$ is an element of the vector $\mathbf{s}^t$ which is a K'-dimensional binary variable having a 1-of-K' representation of brain states at time t. Here, K' is the number of brain states. A particular element $s_{k'}^t$ is equal to 1 and all other elements are equal to 0 so that we see which brain state a participant is in at time t according to which element is nonzero.

2.4. Dataset 1 (gradCPT dataset)

We examined the observed number of brain states during the gradCPT and resting state, and whether performance differed during these distinct brain states. In order to investigate whether local minimum brain states were identical during gradCPT and resting state, energy landscape analysis was performed separately.

2.4.1. Participants and task paradigm

Sixteen participants (6 males, ages 18–34 years, mean age = 24.1 years) performed the gradCPT during fMRI. Subjects completed the three 8 min gradCPT runs and one 6 min resting-state fMRI. The data used in this study and portions of the methods have been published (Esterman et al., 2013), but the current analyses and results have not been published elsewhere. All participants were right-handed, with normal or corrected-to-normal vision and no reported history of major medical illness, head trauma, neurological, or psychiatric disorder. The study was approved by the VA Boston Healthcare System IRB, and written consent was obtained from all participants.

2.4.2. Brain behavior relationship analysis

If brain activity during gradCPT can be described as transitions between behaviorally different attentional states (Esterman et al., 2013) (Fig. 1d), such states should correspond to stable brain states which have local energy minima. After defining local minimum brain activity patterns as brain states, all participants had a brain state transition time series and a behavioral time series. Thus, we calculated behavioral performance during each brain state. We shifted the time labels of the brain states backwards by 5 seconds to account for the hemodynamic response lag.

2.5. Dataset 2 (gradCPT with thought probe dataset)

We attempted to replicate the results in Dataset 1 using an independent dataset. Furthermore, in this dataset we measured self-reported mind-wandering by using intermittent thought-probes and compared the degree of mind wandering between brain states.

2.5.1. Participants and Task paradigm

Twenty-nine participants (13 males, ages 21–36 years, mean age = 26.4 years) performed the long inter-stimulus interval (ISI) gradCPT (1300 ms compared to 800 ms in the Dataset 1) during fMRI. Subjects completed four long-ISI gradCPT runs with intermittent thought-probes. The data used in this study and portions of the methods have been published (Kucyi et al., 2016), but the current analyses and results have not been published elsewhere. Subjects were screened by phone and at an initial visit before the day of neuroimaging, where subjects were also trained on performing the long-ISI gradCPT. Exclusion criteria were as follows: current mood, psychotic, anxiety (excluding simple phobias) or ADHD, current use of psychotropic medication, full-scale IQ less than 80, neurological disorders, sensorimotor handicaps, current alcohol or substance abuse/dependence, and claustrophobia. The study was approved by the Partners Human Research Institutional Review Board, and written consent was obtained from all participants.

Participants performed the gradCPT, modified here to include thought-probes. Thought-probes appeared pseudo-randomly every 44–60 s (three possible block durations of 44, 52, and 60 s). Rather than gradually transitioning into another scene image, the last scene before the thought-probe faded into a scrambled image (to give subjects a similar amount of time to respond as in other trials). Upon the thought-probe, a question was displayed: “To what degree was your focus just on the task or on something else?” A continuous scale appeared below the question text with far-right and far-left anchors of “only task” and “only else”, respectively. Subjects pressed buttons with their middle and ring fingers to move the scale left and right, respectively, and with their thumb to enter their response. Responses were recorded on a graded scale of integers (not visible to the subjects) ranging from 0 (only task) to 100 (only else). A second self-paced question screen about meta-awareness of task-related focus (“To what degree were you aware of where your focus was?”) appeared after the thought-probe, but responses for this second question were not included in the present analyses. The gradCPT immediately resumed after subjects entered their question responses (except for the last thought-probe in the run). Scanning was manually stopped after each gradCPT thought-probe run.

2.5.2. Brain behavior relationship analysis

We applied the identical analysis procedure as in Dataset 1 (see *2.4.3 Brain behavior relationship analysis*). Since mind-wandering was measured intermittently, we estimated the time series of mind-wandering by performing linear interpolation, so that we could calculate mind-wandering during each brain state.

2.6. Dataset 3 (ADHD gradCPT dataset)

We investigated how ADHD impacts the character of the brain states (activity patterns and frequency of these states) and behavioral performance during these states.

2.6.1. Participants and task paradigm

Nineteen adults with ADHD (8 males, ages 18–34 years, mean age = 24 years) also performed the gradCPT during fMRI data collection. The task paradigm was completely same as in Dataset 2 (see *2.5.1 Participants and Task paradigm*). The study was approved by the Partners Human Research Institutional Review Board, and written consent was obtained from all participants.

2.6.2. Brain behavior relationship analysis

We investigated the effect of ADHD. We applied the identical analysis procedure as in Dataset 2 (see *2.5.3 Brain behavior relationship analysis*) to this ADHD dataset. For statistical analysis, we applied a mixed-effects linear regression model to dwell time and behavioral performance with brain state, ADHD (compared to healthy control [HC]), and their interactions, as fixed effects, and subject as a random effect. We used the results of the HCs from Dataset 2 as a comparison, because task paradigms were identical.

2.7. Dataset 4 (gradCPT with reward dataset)

We investigated how motivation impacted the character of the brain states (activity patterns and frequency of these states) and behavioral performance during these states.

2.7.1. Participants and task paradigm

Sixteen participants (10 males, ages = 19–29, mean age = 22 years) completed three to five 8-min runs of the gradCPT (13 participants completed five runs, 2 completed four runs, and 1 completed three runs) during fMRI. The data used in this study and portions of the methods have been published (Esterman et al., 2017a), but the current analyses and results have not been published elsewhere. Fourteen participants were right-handed and all were considered healthy, had normal or corrected-to-normal vision, and no reported history of major illness, head trauma, or neurological/psychiatric disorders. All were screened to confirm no metallic implants or history of claustrophobia. Drug/medication use was not explicitly assessed. The study protocol was approved by the VA Boston Healthcare System Institutional Review Board, and all participants gave written informed consent.

In this dataset, each 8-min task run was divided into alternating 1-min rewarded (motivated) and unrewarded (unmotivated) blocks, which were differentiated by a continuous color border (green for rewarded; blue for unrewarded). To have the background colors be more intuitive and avoid confusion, "green" was chosen for rewarded blocks in all participants rather than counterbalancing green and blue colors. This yielded 4 min of each block-type per run. Similar to our previous study (Esterman et al., 2014a), participants earned $0.01 for correctly pressing to city scenes and $0.10 for correctly withholding a response to mountain scenes during rewarded blocks. However, if a participant failed to press to a city scene, they would lose $0.01, and if a participant incorrectly pressed to a mountain scene, they would lose $0.10. During the unrewarded blocks, no money could be gained or lost. These identical reward contingencies were shown to produce reliable improvements in accuracy and RT variability in a study with 54 participants (Esterman et al., 2014a), and in previously published work with this data (Esterman et al., 2017a), thus *a priori*, we were certain the payoff matrix successfully modulated sustained attention performance.

2.7.2. Brain behavior relationship analysis

First, we aimed to replicate the previous results, using the unmotivated blocks only, as previous datasets included no extrinsic motivation. Next, we investigated how reward-induced motivation affects performance and brain states. Each 8 min task run was divided into alternating 1 min motivated (rewarded) and unmotivated (unrewarded) blocks yielding 4 min of each block-type per run. To investigate whether stable brain states differ between motivated and unmotivated blocks, we divided all BOLD signals during this task into rewarded and unrewarded blocks and concatenated BOLD signals from all participants for each block. We then conducted the energy landscape analysis separately in each block type and investigated the stable brain states. We then calculated behavioral performance during each brain state for each block type separately. We shifted the time labels of the brain states backwards by 5 s to account for the hemodynamic response. For statistical analysis, we applied a mixed-effects linear regression model to dwell time and behavioral performance with brain state, reward/nonreward, and their interaction as fixed effects, and subject as a random effect.

3. Results

3.1. Local energy minimum brain states during gradual onset continuous performance task (Dataset 1)

First, we confirmed the pairwise MEM accurately fit the data (Supplementary Figure 1). This result indicates that estimation of energy in each brain activity pattern was accurate. Next, based on this MEM, two local minimum brain states were identified during the gradCPT and resting state. Fig.2a (left) shows the brain activity patterns in the 7 networks for the 2 local minimum brain states and Fig. 2a (right) shows the percentage of dwell time for each state during the gradCPT. One state (State1) was characterized as activation of the DMN and limbic networks, and the other state (State2) was characterized as activation of frontoparietal network (FPN), DAN, SAN, somato-motor (SMN) and visual networks. Fig. 2b (left) shows the brain activity patterns in the 7 networks for the 2 local minimum brain states and Fig. 2b (right) shows the percentage of dwell time for each state during resting state. The first state (State1) was characterized as activation of DMN, FPN, and limbic networks and the other state (State2) was characterized as activation of DAN, SAN, SMN and visual networks. We found that participants spent more time in State2 during gradCPT than in State1 and more time in State1 during rest than in State2 (gradCPT: t_{15}= 2.17, P = 0.046, effect size (Hedges's g) = 0.54; rest: t_{15}= 3.92, P = 0.0014, effect size (Hedges's g) = 0.98, paired t-test for dwell time in State1 and State2).

Only the FPN activation was different between states during the gradCPT and during rest. Although we found 2 local minimum brain states in both the gradCPT and rest, activation of the FPN differed. We consider whether this difference is meaningful in a follow up analysis (*3.4 Follow up analysis of FPN in brain states*). Furthermore, we investigated the dwell time of individual activity patterns in each brain state. We found that the local minimum brain activity pattern had the longest or 2nd longest dwell time in both brain states (Supplementary Figure 2).

We confirmed two dominant brain states were robust to choice of ROIs (Supplementary Figures 3) (Power et al., 2011; Schaefer et al., 2018). For example, when we used the Power's 264 ROIs categorized by 14 networks and conducted the identical procedure (see *2.3 fMRI analysis*), we found six local minimum brain states and two of them were dominant during the gradCPT (the percentages of dwell time in both brain states were over 40%) (Supplementary Fig. 3). We found these two dominant states were similar to the brain states using Schaefer's atlas. One state was characterized as activation of the DMN, memory retrieval network, and "uncertain" and was similar to State1 in Schaefer's atlas. The other state was characterized as activation of cerebellar, cingulo-opecular, DAN, FPN, SAN, SMN, subcortical, ventral attention, and visual networks and was similar to State2 in Schaefer's atlas. Furthermore, in the current analysis we calculated 7 network time series by averaging BOLD signal time courses at the ROI-level following the procedure in previous work (Watanabe and Rees, 2017). We also calculated the 7 network time series by averaging the BOLD signal time courses for the voxel level. The results were almost identical as those in the main text. These results indicate that fluctuations of brain activity can be described as dynamic transitions between two dominant brain states.

We then examined behavioral differences in performance between State1 and State2. We focused on variables commonly used to assess the optimality of sustained attention, including reaction time variability, reaction time, and accuracy (d prime) as measures of performance. We found that d prime was significantly higher during State1 than during State2 (paired t-test. Reaction time variability: t_{15}= 1.55, P = 0.14, effect size (Hedges's g) = 0.39; Mean reaction time: t_{15}= 1.26, P = 0.23, effect size (Hedges's g) = 0.31; d prime: t_{15}= 3.24, P = 0.0055, effect size (Hedges's g) = 0.81, two-sided without correction for multiple comparisons) (Fig. 2c–e). This result indicates that participants maintained more accurate performance during State1 than those during State2. Furthermore, we confirmed that the behavioral differences in performances between the states were robust to our choice of ROIs (Supplementary Figure 3).

3.2. Replication and investigation of mind wandering (Dataset 2)

Next, we attempted to replicate the results in Dataset 1 using an independent dataset (Dataset 2) and investigate whether the degree of mind wandering differed between brain states. First, we confirmed the pairwise MEM accurately fit to the data (Supplementary Figure 1). This result indicates that estimation of energy in each brain activity pattern was accurate. Again, we found two local minimum brain states in this independent gradCPT dataset (Fig. 3a). Generally consistent with the previous dataset, one state was characterized as activation of DMN, FPN, and limbic networks (State1) and the other state was characterized as

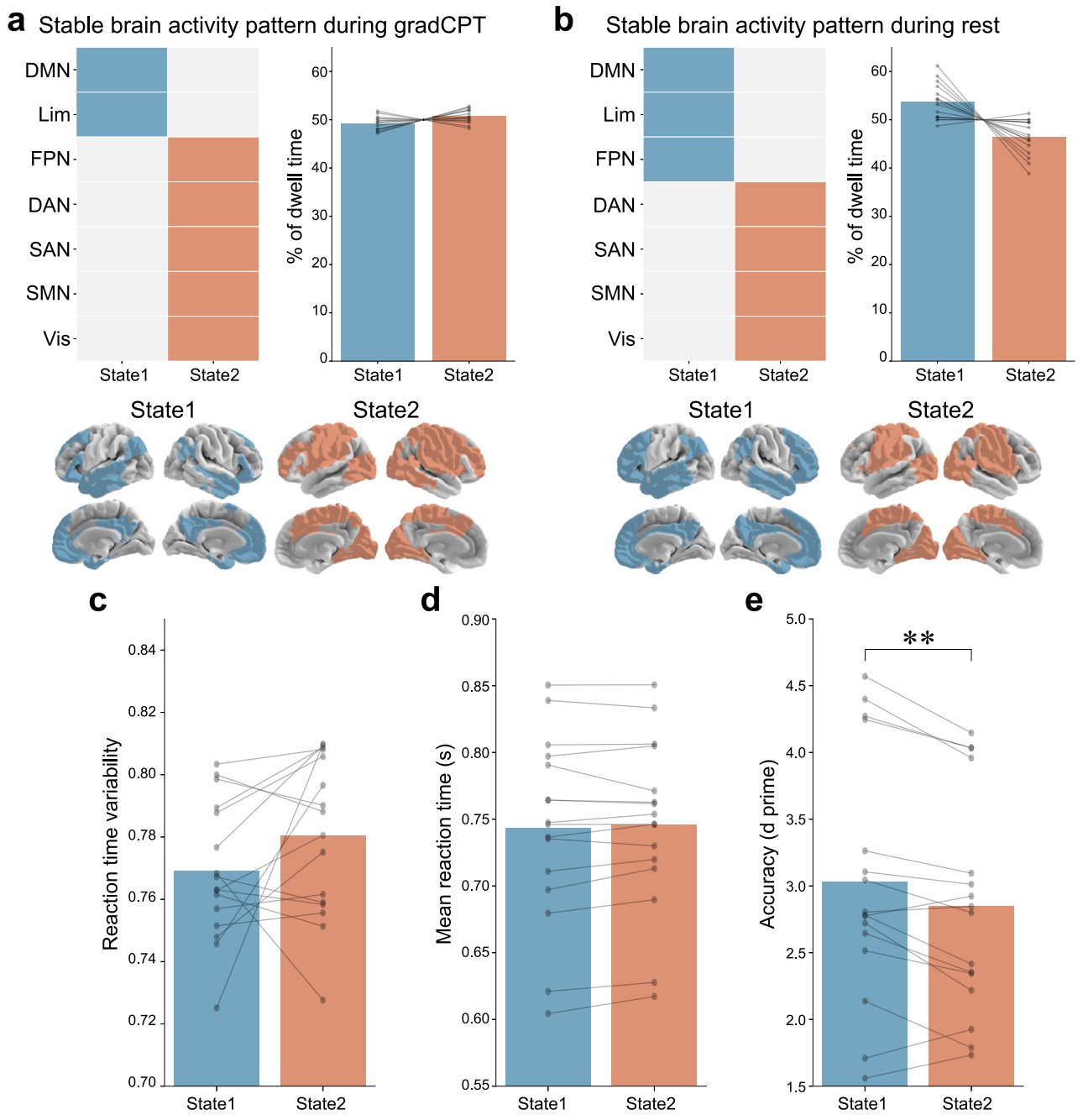

Fig. 2. Energetically stable brain states and behavioral performance during these states. (a) Stable brain states during gradual onset continuous performance task (gradCPT). Individual state is represented by an activity pattern in which each brain region is active (blue and red) or inactive (white). Bar graph shows the percentage of dwell time during gradCPT in each individual state. Blue bar shows State1 and red bar shows State2. Each scatter shows each participant. Brain images indicate brain activation in each brain state. (b) Stable brain states during rest. Bar graph shows percentage of dwell time during rest in each individual state. Brain images indicates brain activation in both brain states. (c–e) Behavioral performance in each brain state during gradCPT. (c) Reaction time variability. (d) Mean reaction time. (e) Accuracy (d prime). Each scatter shows each participant and lines connect the same participant. $^{**}P < 0.01$. DMN: default mode network; Lim: limbic; FPN: frontoparietal network; DAN: dorsal attention network; SAN: salience network; SMN: somatomotor network; Vis: visual.

activation of DAN, SAN, SMN and visual networks (State2). We found that participants spend more time in State1 than in State2 (t_{28}= 3.30, P = 0.0026, effect size (Hedges's g) = 0.61, paired t-test for dwell time in State1 and State2, data shown in Fig 4b [HC]).

Furthermore, we found that behavioral performance was significantly different between State1 and State2, such that performance in State1 was more accurate, as well as faster and less variable (paired t-test. Reaction time variability: t_{28}= 5.01, $P = 2.7 \times 10^{-5}$, effect size (Hedges's g) = 0.93; Mean reaction time: t_{28}= 5.90, $P = 2.4 \times 10^{-6}$, effect size (Hedges's g) = 1.09; d prime: t_{28}= 4.60, $P = 8.3 \times 10^{-5}$, effect size (Hedges's g) = 0.85, two-sided without correction for multiple comparisons; Fig. 3b-d). Despite better performance, the degree of mind wandering was higher in State1 (Mind wandering score: t_{28}= 4.31, P = 0.00018, effect size (Hedges's g) = 0.80; Fig. 3e). Although we found

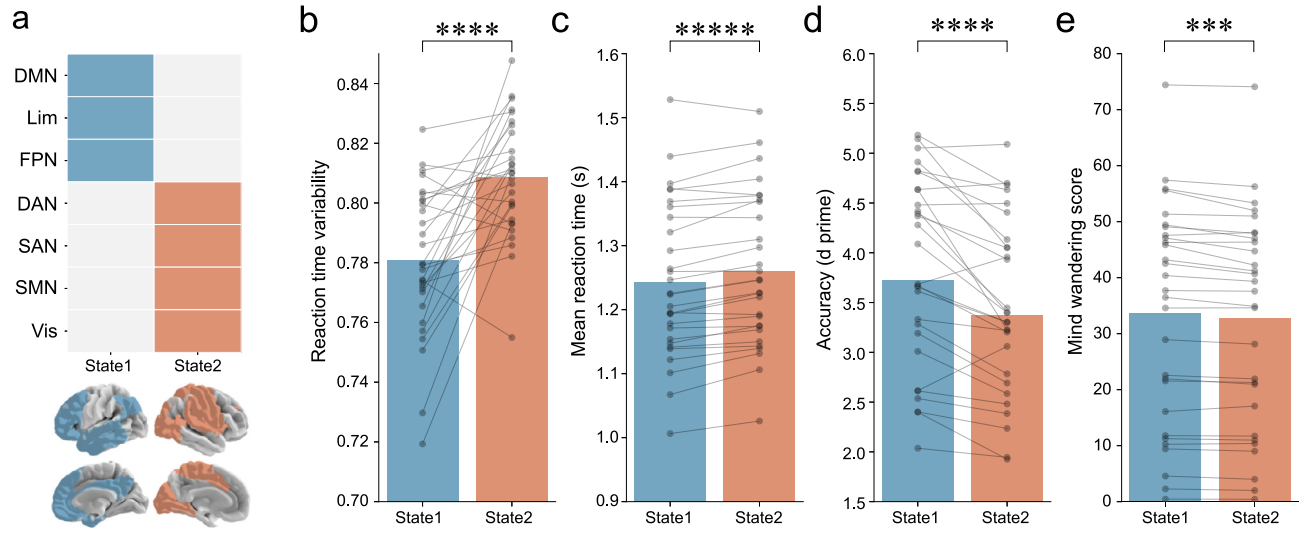

Fig. 3. Replication and mind wandering difference between brain states. (a) Stable brain states during gradual onset continuous performance task (gradCPT). Individual state is represented by an activity pattern in which each brain region is active (blue and red) or inactive (white). Brain images indicate brain activation in each brain state. (b–e) Behavioral performance in each brain states during the gradCPT. (b) Reaction time variability. (c) Mean reaction time. (d) Accuracy (d prime). (e) Mind wandering score. Each scatter shows each participant and lines connect the same participant. $^{***}P < 0.001$, $^{****}P < 10^{-4}$, $^{*****}P < 10^{-5}$. DMN: default mode network; Lim: limbic; FPN: frontoparietal network; DAN: dorsal attention network; SAN: salience network; SMN: somatomotor network; Vis: visual.

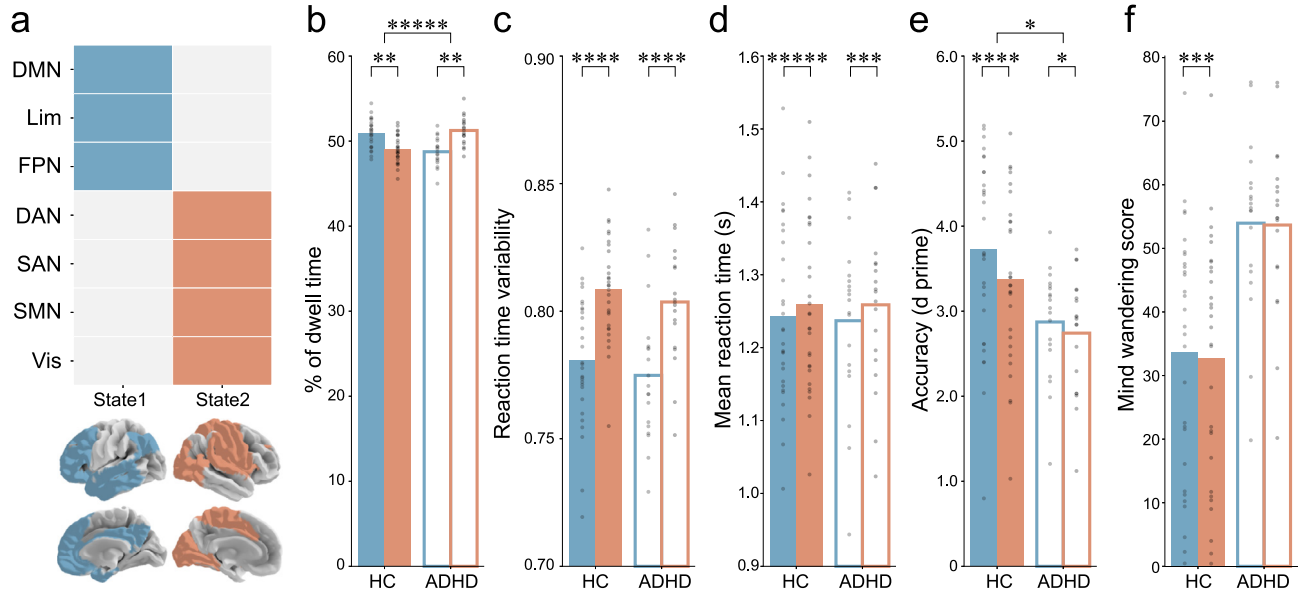

Fig. 4. Effect of ADHD on dwell time and behavioral performance. (a) Stable brain states during gradual onset continuous performance task (gradCPT). The individual state is represented by an activity pattern in which each brain region is active (blue and red) or inactive (white). Brain images indicate brain activation in each brain state. (b) Percentage of dwell time in each brain state during gradCPT. (c–f) Behavioral performance in each brain state during the gradCPT. (c) Reaction time variability. (d) Mean reaction time. (e) Accuracy (d prime). (f) Mind wandering score. Filled bar graph shows the results in healthy control and edge bar graph shows the results in ADHD. Each scatter shows each participant. $^{*}P < 0.05$, $^{*}P < 0.01$, $^{***}P < 0.001$, $^{****}P < 10^{-4}$, $^{*****}P < 10^{-5}$. DMN: default mode network; Lim: limbic; FPN: frontoparietal network; DAN: dorsal attention network; SAN: salience network; SMN: somatomotor network; Vis: visual; HC: healthy control; ADHD: attention-deficit hyperactivity disorder

nearly the same 2 local minimum brain states in this dataset compared to Dataset 1 during the gradCPT, activation of FPN was found in State1 (whereas FPN activation was associated with State2 in Dataset 1 during the gradCPT). We further consider this difference in a follow up analyses (*3.4 Follow up analysis of FPN in brain states*).

3.3. Investigating the influence of additional cognitive and clinical factors

Next, we investigated how ADHD and motivation affected sustained attention and the characteristics of these brain states. There are four possibilities for the impact of these factors: (1) the factor directly impacts the nature of the brain state(s) (alters the brain activity pattern of brain state), (2) the factor impacts the dwell time in the brain state(s), (3) the factor impacts performance across both brain states equally, (4) the factor impacts performance differentially in one brain state.

3.3.1. Influence of ADHD (Dataset 3)

First, we confirmed the pairwise MEM accurately fit the data (Supplementary Figure 1). This result indicates that the estimation of energy in each brain activity pattern was accurate. We again found two dom-

inant brain states even in the ADHD dataset (Fig. 4a). One state was characterized as activation of DMN, FPN, and limbic networks (State1) and the other state was characterized as activation of DAN, SAN, SMN and visual networks (State2).

We replicated the difference in behavioral performance during State1 and State2 in the ADHD dataset, demonstrating more accurate, as well as faster and less variable reaction times in State1 compared to State2 (paired *t*-test. Reaction time variability: t_{18}= 5.50, $P = 3.2 \times 10^{-5}$, effect size (Hedges's *g*) = 1.26; Mean reaction time: t_{18}= 4.61, $P = 0.0022$, effect size (Hedges's *g*) = 1.06; d prime: t_{18}= 2.26, $P = 0.037$, effect size (Hedges's *g*) = 0.52, two-sided without correction for multiple comparisons). However, we did not find significant difference in the mind wandering score between states (t_{18}= 1.23, $P = 0.24$, effect size (Hedges's *g*) = 0.28, two-sided without correction for multiple comparisons).

Using Dataset 2 (HC controls) acs a comparison group, we investigated the interaction effect between group (HC and ADHD) and brain state. We found a significant interaction for dwell time and d prime (Mixed effects model interaction effects between brain state and group: Dwell time: $t_{92} = 6.75$, $P = 1.02 \times 10^{-9}$, $P_{FDR} = 5.10 \times 10^{-9}$, effect size (Cohen's f^2) = 0.47; d prime: $t_{92} = 2.15$, $P = 0.036$, $P_{FDR} = 0.089$, effect size (Cohen's f^2) = 0.11, *t*-test on mixed effects model) (Fig. 4). On the one hand, HCs spend significantly more time in State1 than in State2 (paired *t*-test. t_{28}= 3.30, $P = 0.0026$, effect size (Hedges's *g*) = 1.23). On the other hand, individuals with ADHD spend significantly more time in State2 than in State1 (paired *t*-test. t_{18}= 3.31, $P = 0.0039$, effect size (Hedges's *g*) = 0.76). The interaction effect (state x group) for d prime indicates that while both groups show accuracy differences between State1 and State2, this effect is muted in participants with ADHD (Fig. 4e). Of note, the interaction effect for d prime must be interpreted with caution, because it is not significant ($P = 0.089$) after correction for multiple comparisons.

3.3.2. Influence of motivation (Dataset 4)

First, we confirmed the pairwise MEM accurately fit to the data (Supplementary Figure 1) in both blocks. This result indicates that estimation of energy in each brain activity pattern was accurate. As found in previous analyses, same two dominant brain states were observed for both block types (Fig. 5a). One state was characterized as activation of DMN, FPN, and limbic networks (State1) and the other state was characterized as activation of DAN, SAN, SMN and visual networks (State2).

We first verified whether the relationship between brain states and behavior could be replicated when using only unmotivated block data, akin to previous analyses (all without reward). Note that the unmotivated block data are not identical to other datasets because the unmotivated blocks might be actively de-motivated by the presence of the motivated blocks. However, we successfully replicated the difference in performance between states (paired *t*-test. Reaction time variability: t_{15}= 4.62, $P = 0.00033$, effect size (Hedges's *g*) = 1.15; Mean reaction time: t_{15}= 5.25, $P = 9.8 \times 10^{-5}$, effect size (Hedges's *g*) = 1.31; d prime: t_{15}= 4.43, $P = 0.00049$, effect size (Hedges's *g*) = 1.11, two-sided without correction for multiple comparisons) (Fig. 5 pale color).

We then investigated whether there were significant interactions between brain state and motivation for dwell time and behavioral performance. We found a significant interaction effect for dwell time as well as d prime (Mixed effects model interaction effect between brain state and motivation: Dwell time: $t_{60} = 4.59$, $P = 2.0 \times 10^{-5}$, $P_{FDR} = 7.9 \times 10^{-5}$, effect size (Cohen's f^2) = 0.33; d prime: $t_{60} = 2.16$, $P = 0.035$, $P_{FDR} = 0.069$, effect size (Cohen's f^2) = 0.11, *t*-test on mixed effects model) (Fig. 5). We found that participants spend more time in State2 during motivated blocks and less time in State1 during unmotivated blocks (t_{15}= 2.90, $P = 0.011$, effect size (Hedges's *g*) = 0.72, paired *t*-test for dwell time in State1 between unmotivated and motivated blocks). Although we found a significant difference in d prime between brain states during the unmotivated blocks, we did not find significant differences in d prime during motivated blocks (Unmotivated block: t_{15}= 4.43, $P = 0.00049$, effect size (Hedges's *g*) = 1.11, Motivated block: t_{15} = 1.14, $P = 0.27$, effect size (Hedges's *g*) = 0.28). This indicates that while motivation increased dwell time in State2, it overcame the decreased accuracy associated with State2. Of note, the interaction effect for d prime (accuracy) must be interpreted with caution, because it is not significant ($P = 0.069$) after correction for multiple comparisons.

3.4. Follow up analysis of FPN in brain states

In Dataset 1, FPN was inactive in State1 and active in State2 during the gradCPT. For resting state and the other 3 datasets, FPN was active in State1 and not State2. Nevertheless, state composition and behavioral correlates were quite similar across all datasets. To better evaluate the discrepant FPN results, we compared the energy value between the adjacent states with and without active FPN across all datasets and we did not find any significant difference (paired *t*-test. State1: t_5= 1.92, $P = 0.11$, effect size (Hedges's g) = 0.77; State2: t_5= 0.49, $P = 0.64$, effect size (Hedges's g) = 0.20; Supplementary Fig. 4). This result indicates that the local minima, and thus stable brain State1 and State2 were agnostic to the activation of FPN.

Furthermore, a recent study identified two distinct subsystems within the FPN. FPN_A exhibited stronger connectivity with the DMN than the DAN, whereas FPN_B exhibited the opposite pattern (Dixon et al., 2018). Thus, we then split the FPN into FPN_A and FPN_B using Yeo's 17 network (Schaefer et al., 2018) and applied the energy landscape analysis to Dataset 1 and Dataset 2 again. As a result, we found the exact same two brain states in both datasets with FPN_A assigned to State1 and FPN_B assigned to State2. Supplementary Figure 5 shows the brain map of FPN_A and FPN_B, and the difference in behavioral performance between brain states in Dataset 2. These results indicate that FPN's subsystem, FPN_A, is active in State1, and FPN_B is active in State2. That is, the discrepant FPN results could be explained by subsystems of the FPN.

4. Discussion

In the present study, we repeatedly demonstrated the ability to detect behaviorally-relevant brain states, on the basis of brain activity alone, agnostic to behavior. Specifically, we consistently observed two dominant brain states during sustained attention in all four datasets. One state was consistently characterized by activation of DMN and limbic networks (State1), and the other state was consistently characterized by activation of DAN, SAN, SMN and visual networks (State2). During the former state, reaction time variability was lower, reaction times were faster, and accuracy was higher, but degree of mind wandering was also higher. During the latter state, reaction time variability was higher, reaction time was slower, and accuracy was lower, but degree of mind wandering was lower. We replicated these results in multiple independent datasets, indicating that State1 was objectively behaviorally optimal and State2 was behaviorally suboptimal. Furthermore, we found that ADHD altered the dwell time by decreasing the time spent in optimal State1 and by increasing the time spent in suboptimal State2 relative to healthy controls. ADHD also reduced the impact of brain state on accuracy. Finally, we revealed the impact of motivation, which altered the brain states' characteristics by overcoming the suboptimal nature of State2, as well as increasing the dwell time spent in that state.

Our results provided evidence that it is possible to define attentional states independently from behavior. This enabled us to estimate subjects' attentional states from brain activity without requiring overt responses from subjects. Since it is relatively difficult to get frequent and continuous behavior from many naturalistic tasks, as well as from some patient populations, our attentional states defined by brain activity enhance the ability to track hidden states of attention and could help better reveal neurobiological mechanisms underlying disorders of attention. Although we found the same brain states even during resting state, our

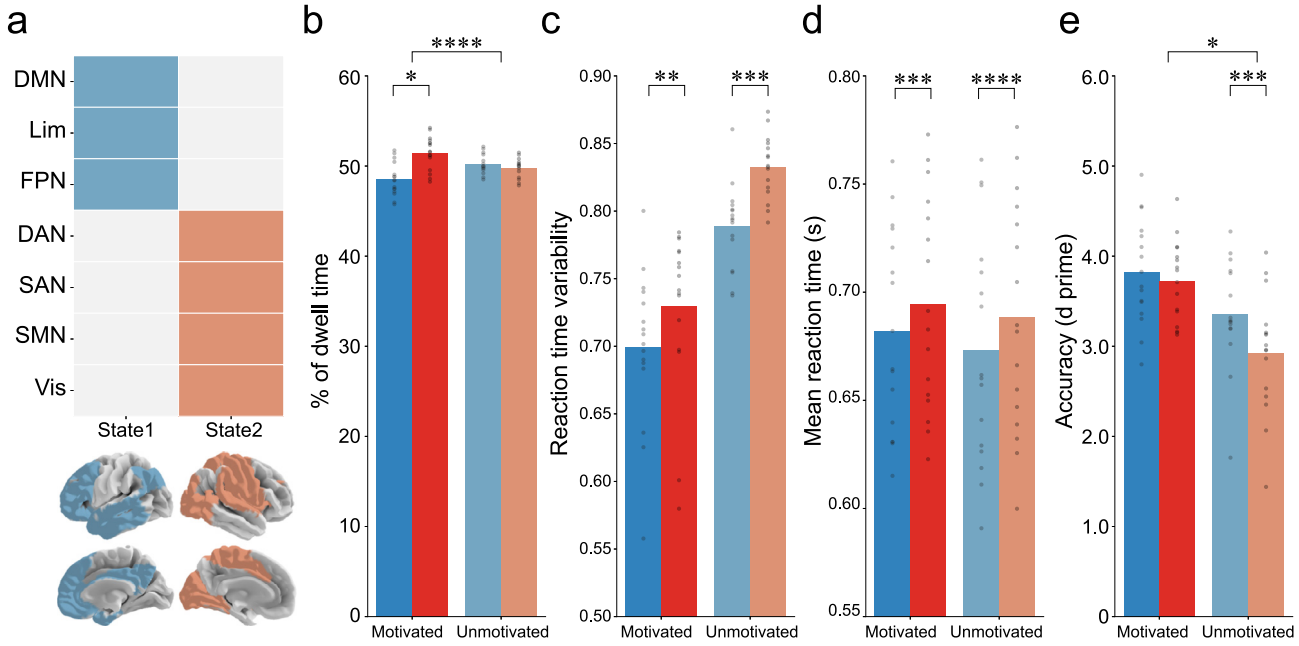

Fig. 5. Effect of motivation on dwell time and behavioral performance. (a) Stable brain states during gradual onset continuous performance task (gradCPT). Individual states are represented by an activity pattern in which each brain region is active (blue and red) or inactive (white). Brain images indicate brain activation in each brain state. (b) Percentage of dwell time in each brain state during gradCPT. (c–e) Behavioral performance in each brain state during gradCPT. (c) Reaction time variability. (d) Mean reaction time. (e) Accuracy (d prime). Dark color bar graph shows the results in motivated block and pale color bar graphs shows the results in unmotivated block. Each scatter shows each participant. $^{*}P < 0.05$, $^{*}P < 0.01$, $^{***}P < 0.001$, $^{****}P < 10^{-4}$. DMN: default mode network; Lim: limbic; FPN: frontoparietal network; DAN: dorsal attention network; SAN: salience network; SMN: somatomotor network; Vis: visual.

current results are heavily reliant on a specific task (gradCPT). The generalization of our results to the other cognitive tasks is an open question. Notably, a previous study identified a whole-brain network architecture present across dozens of task states that was highly similar to the resting state network architecture (Cole et al., 2014). Together, these data suggest that observed brain states could generalize to other cognitive tasks and conditions. Even if the brain states are consistently present, performance differences between states may differ for other cognitive tasks.

In this study, behavioral performance was consistently better (lower reaction time variability and higher accuracy) during the state characterized as activation of DMN and limbic networks than during the state characterized as activation of DAN, SAN, SMN and visual networks. It is interesting to note that these two brain activity patterns are similar to what a previous study has called the dual intertwined rings architecture (Mesmoudi et al., 2013). This "dual intertwined architecture" suggests that the one ring similar to our State2 performs real-time multimodal integration of sensorimotor information whereas the other ring similar to our State1 performs multi-temporal integration. Furthermore, this brain activity pattern is consistent with several other studies from our lab and others demonstrating DMN activity associated with response stability and high accuracy, and DAN/SAN associated with response instability and low accuracy, when states were defined behaviorally (Esterman et al., 2013; Esterman et al., 2017a; Esterman et al., 2014b; Fortenbaugh et al., 2018; Kucyi et al., 2017). Previously, we have referred to periods of response stability as "in-the-zone" states and periods of response instability as "out-of-the-zone" states and have characterized brain differences between these states (Esterman et al., 2013; Esterman et al., 2017a; Esterman et al., 2014b; Kucyi et al., 2016; Rosenberg et al., 2013; Rothlein et al., 2018). As "in the zone" state may reflect automated, and more efficient visual information processing (Esterman et al., 2014b; Rothlein et al., 2018; Vatansever et al., 2017), the brain state associated with better performance identified in this study may have captured this experience. On the other hand, since DMN activity can typically represents "off-task" thoughts and is related to mind wandering (Mason et al., 2007), DMN activity can also have a negative impact on performance (Hinds et al., 2013; Weissman et al., 2006). However, previous studies showed that such relationships are highly complex, such that spontaneous DMN activity can be simultaneously related to both mind wandering and stable "in the zone" performance (Kucyi et al., 2016). This result indicates that there are multiple possible cognitive processes/operations associated with DMN activity. Consistent with this idea, our results found that the degree of mind wandering was significantly higher during the more optimal DMN state than the other state, suggesting that the difference in behavioral performance between the two dominant states could be due to largely distinct mechanisms from mind wandering. Regarding the contribution of FPN, a recent study identified two distinct subsystems within the FPN. FPN_A exhibited stronger connectivity with the DMN than the DAN, whereas FPN_B exhibited the opposite pattern (Dixon et al., 2018). In our brain states, subsystem FPN_A was assigned to State1 where DMN is active, and subsystem FPN_B was assigned to State2 where DAN is active. Previous studies indicate that FPN relates to both executive control/attention networks (State2) (Gratton et al., 2018; Spreng et al., 2013), as well as mind wandering/DMN (State1) (Fox et al., 2015; Stawarczyk and D'Argembeau, 2015), and that the differences in these roles may be due to differences in the FPN subsystems.

Many previous studies have examined differences in brain activity when behavioral performance was better or worse, without considering the connectome (Esterman et al., 2013; Hinds et al., 2013; Thompson et al., 2013; Weissman et al., 2006). Studies have also examined the relationship between individual differences in the connectome between functionally different intrinsic brain networks and sustained attention performance, without considering the brain activity pattern (Kelly et al., 2008; Rosenberg et al., 2016a; Rothlein et al., 2018; Thompson et al., 2013). Recent work has also shown that within-subject attentional fluctuations vary with DAN-DMN connectivity as well as multivoxel information processing-based measures involving those networks (Rothlein et al., 2018). However, whether and how the connectome relates to sustained attention through the intermediary of their

brain activity has remained unclear (Mill et al., 2017). Our energy landscape model clarified this relationship, as it indicates that brain activity during sustained attention tasks can be described as a series of stays and transitions between two dominant attractors (brain states) with different attentional performance on the energy landscape, and such attractors are constrained by the brain's intrinsic connectome.

We found that individuals with ADHD spent less time in the optimal brain state associated with better performance (low reaction time variability and high accuracy) than healthy controls. While several relationships between brain states and behavioral performance were comparable across groups, individuals with ADHD had lower accuracy and higher mind wandering scores regardless of the brain state (Fig. 4e and f). This result indicates that the difference in spent time in the optimal brain state may partially explain the neural mechanism of attentional deficits in ADHD, in that an optimal and efficient brain state may be less "energetically" stable. Furthermore, the interaction effect between state and dprime indicates that individuals with ADHD may show a muted positive impact of the optimal state on performance (or alternatively a smaller negative impact of the suboptimal state) than in HCs.

Our results also showed that although participants spend more time in the brain state associated with worse performance (high RT variability and low accuracy) during motivated blocks, motivation simultaneously partially overcame the negative impact of this state on performance. This disparate result may be explained by the difference between proactive and reactive activation of DAN (and SAN), such that proactive engagement of the goal-oriented DAN may support better performance, but reactive activation of this network may represent a response to errors or periods of struggle and thus less efficient engagement (Esterman et al., 2017a). Interestingly, our results showed that motivation improves d-prime but does not decrease RT variability in the suboptimal state. This suggests that motivation affects cognitive performance via different neural mechanisms (e.g. via effects on the visual system rather than the motor system). These results indicate that it is possible to consider State2 to be a cognitively effortful state, and that reward increased the cognitive effort and partially overcame the negative effects of this brain state on performance. Conversely, this result also shows that reward did not increase spend time in the brain state associated with more automated information processing (State1). According to a previous study, the automated information processing could be achieved by learning via such mechanisms as repeating tasks (Vatansever et al., 2017). Therefore, future work could investigate the increase of time spent in State1 related to automated information processing by examining learning and repeated task practice. From the view point of information processing between brain regions, our previous study showed the effects of motivation on information processing were orthogonal to intrinsic fluctuations of attention, such that there was increased communication of stimulus information between the DAN and DMN during the motivated block (Rothlein et al., 2018). Furthermore, another study suggests that motivation may help improve task performance by reducing the depth of mind wandering, while also providing insulation from the negative effects of mind wandering, when it does occur (Brosowsky et al., 2020). Further study is needed to clarify the effect of motivation. For example, it may be possible to more specifically explore how neural measures of information processing change in different brain states as compared to motivational states, in conjunction with other factors such as mind wandering and arousal, which could mediate the effects of motivation (Esterman and Rothlein, 2019).

The energy landscape created in this study is a type of generative model. Generative models enable us to simulate a transition of brain state when brain networks change (e.g. simulation of drug or connectivity neurofeedback effect) or activity of specific brain regions are inhibited or activated (e.g. simulation of brain stimulation)(Esterman et al., 2017b; Rosenberg et al., 2016b; Yamashita et al., 2017). Therefore, in future studies it may be possible to determine optimal targets for neurofeedback and brain stimulation to efficiently remediate and improve sustained attention ability by using our model to optimally change brain states online (deBettencourt et al., 2015; deBettencourt et al., 2019; Esterman et al., 2017b; Yamashita et al., 2017).

Although it was not predetermined, we found only two brain states. Therefore, our results are consistent with a one-to-one correspondence between behavior and brain state, as had been "predetermined" by the analytic approach in previous studies (dichotomizing behavioral states and examining neural correlates). A limitation of our study is the coarse representation of brain states required for the energy landscape analysis. First, since the brain regions used in the current study are network level, it may be possible to define the brain state more flexibly by using finer parcellations. Second, although we assumed that brain networks themselves are stable, the brain networks themselves could change dynamically. Recent work suggested a relationship between dynamic functional connectivity and attentional states, thus networks themselves may reconfigure with attentional fluctuations (Fong et al., 2019; Kucyi et al., 2017). Third, since energy landscape analysis requires the binarization of brain activity into active or inactive, the information about the degree of intensity in brain activation is lost. To overcome these limitations, novel unsupervised learning techniques, based on Bayesian switching linear dynamical systems (BSDS), can provide an integrated framework for identifying latent brain states and dynamic brain connectivity during cognitive tasks (Taghia et al., 2018) more flexibly. Finally, we did not consider what information is processed between brain regions. Recently developed tools to investigate how information transfer between brain regions may allow us to go beyond an assessment of functional connectivity (Anzellotti and Coutanche, 2018; Rothlein et al., 2018). In the future, such advanced techniques could be used to investigate brain states that take into account dynamic functional connectivity and information processing between brain regions, which may further specify the relationship between brain states and cognition.

5. Conclusion

In summary, our study is the first to provide evidence for two attentional states from the sole viewpoint of brain activity, one behaviorally optimal, the other suboptimal. Additionally, our study shows that these brain states are reflected in activity patterns across functionally different brain networks, linking activity and connectivity to sustained attention. Our results revealed that individuals with ADHD spend more time in the suboptimal brain state and less time in the optimal brain state than do HCs. Furthermore, our results suggest that motivation increases cognitive effort and partially overcomes the negative effect of the suboptimal brain state on performance. We believe this approach has wide ranging implications for neurocognitive and clinical models of attention, and can set a new methodological and theoretical trajectory for a wealth of future studies.

Declaration of Competing Interest

The authors declare no competing financial interests.

Data and code availability

Analysis code and summary data required to reproduce all figures in our manuscript is publically available (https://github.com/Ayumu722/BrainStateSustainedAttention). However, a portion of the raw data (e.g. brain images) are owned by the United States Department of Veterans Affairs and are available only upon request from the United States Department of Veterans Affairs. The Department of Veterans Affairs will make this data publicly available and requests for the data can be made by interested individuals by filing a Freedom of Information Act request to the Privacy Officer at VA Boston Healthcare System (vhabhsFOIAofficers@va. gov) or the FOIA Intake Center (see http://www.oprm.va.gov/foia/foia_howTo.aspx for more details).

Funding grants

This research was supported by the TOYOBO Biotechnology Foundation and Overseas Research Fellow in Japan Society for the Promotion of Science to AY and a Merit Review Award from the Department of Veterans Affairs Clinical Sciences Research and Development (I01CX001653) to ME.

Author contributions

M.E., E.V. and A.K. designed the study and recruited participants for the study, collected their clinical and imaging data. A.Y. performed data preprocessing and analysis; A.Y., D.R., and M.E. primarily wrote the manuscript.

Conflict of interest statement

The authors declare no competing financial interests.

Supplementary materials

Supplementary material associated with this article can be found, in the online version, at doi:10.1016/j.neuroimage.2021.118072.

Credit authorship contribution statement

Ayumu Yamashita: Conceptualization, Methodology, Software, Validation, Formal analysis, Investigation, Data curtion, Writing – original draft, Visualization, Project administration, Funding acquisition. **David Rothlein:** Writing – original draft, Data curtion. **Aaron Kucyi:** Writing – review & editing, Resources. **Eve M. Valera:** Writing – review & editing, Resources, Funding acquisition. **Michael Esterman:** Writing – original draft, Supervision, Resources, Funding acquisition.

References

Anzellotti, S., Coutanche, M.N., 2018. Beyond functional connectivity: investigating networks of multivariate representations. Trends Cogn Sci 22, 258–269.
Behzadi, Y., Restom, K., Liau, J., Liu, T.T., 2007. A component based noise correction method (CompCor) for BOLD and perfusion based fMRI. Neuroimage 37, 90–101.
Benjamini, Y., Hochberg, Y., 1995. Controlling the false discovery rate: a practical and powerful approach to multiple testing. J. Roy. Statist. Soc. Ser. A 57, 289–300.
Benjamini, Y., Yekutieli, D., 2001. The control of the false discovery rate in multiple testing under dependency. Ann. Stat. 1165–1188.
Benjamini, Y., Yekutieli, D., 2005. False discovery rate–adjusted multiple confidence intervals for selected parameters. J. Am. Statist. Assoc. 100, 71–81.
Bonett, D.G., 2009. Meta-analytic interval estimation for standardized and unstandardized mean differences. Psychol. Methods 14, 225–238.
Brosowsky, N.P., DeGutis, J., Esterman, M., Smilek, D., Seli, P., 2020. Mind wandering, motivation, and task performance over time: Evidence that motivation insulates people from the negative effects of mind wandering. Psychology of Consciousness: Theory, Research, and Practice. No Pagination Specified-No Pagination Specified.
Castellanos, F.X., Sonuga-Barke, E.J., Milham, M.P., Tannock, R., 2006. Characterizing cognition in ADHD: beyond executive dysfunction. Trends Cogn. Sci. 10, 117–123.
Castellanos, F.X., Tannock, R., 2002. Neuroscience of attention-deficit/hyperactivity disorder: the search for endophenotypes. Nat. Rev. Neurosci. 3, 617–628.
Cheyne, J.A., Solman, G.J., Carriere, J.S., Smilek, D., 2009. Anatomy of an error: A bidirectional state model of task engagement/disengagement and attention-related errors. Cognition 111, 98–113.
Christoff, K., Gordon, A.M., Smallwood, J., Smith, R., Schooler, J.W., 2009. Experience sampling during fMRI reveals default network and executive system contributions to mind wandering. Proc. Natl. Acad. Sci. U S A 106, 8719–8724.
Chun, M.M., Golomb, J.D., Turk-Browne, N.B., 2011. A taxonomy of external and internal attention. Ann. Rev. Psychol. 62, 73–101.
Cole, M.W., Bassett, D.S., Power, J.D., Braver, T.S., Petersen, S.E., 2014. Intrinsic and task-evoked network architectures of the human brain. Neuron 83, 238–251.
deBettencourt, M.T., Cohen, J.D., Lee, R.F., Norman, K.A., Turk-Browne, N.B., 2015. Closed-loop training of attention with real-time brain imaging. Nat. Neurosci. 18, 470–475.
deBettencourt, M.T., Keene, P.A., Awh, E., Vogel, E.K., 2019. Real-time triggering reveals concurrent lapses of attention and working memory. Nat. Hum. Behav. 3, 808–816.
Deco, G., Rolls, E.T., Romo, R., 2009. Stochastic dynamics as a principle of brain function. Prog. Neurobiol. 88, 1–16.
Deco, G., Senden, M., Jirsa, V., 2012. How anatomy shapes dynamics: a semi-analytical study of the brain at rest by a simple spin model. Front. Comput. Neurosci. 6, 68.
Di Martino, A., Ghaffari, M., Curchack, J., Reiss, P., Hyde, C., Vannucci, M., Petkova, E., Klein, D.F., Castellanos, F.X., 2008. Decomposing intra-subject variability in children with attention-deficit/hyperactivity disorder. Biol. Psychiatry 64, 607–614.
Dixon, M.L., De La Vega, A., Mills, C., Andrews-Hanna, J., Spreng, R.N., Cole, M.W., Christoff, K., 2018. Heterogeneity within the frontoparietal control network and its relationship to the default and dorsal attention networks. Proc. Natl. Acad. Sci. 115, E1598–E1607.
Drummond, S.P., Bischoff-Grethe, A., Dinges, D.F., Ayalon, L., Mednick, S.C., Meloy, M.J., 2005. The neural basis of the psychomotor vigilance task. Sleep 28, 1059–1068.
Esteban, O., Markiewicz, C.J., Blair, R.W., Moodie, C.A., Isik, A.I., Erramuzpe, A., Kent, J.D., Goncalves, M., DuPre, E., Snyder, M., Oya, H., Ghosh, S.S., Wright, J., Durnez, J., Poldrack, R.A., Gorgolewski, K.J., 2019. fMRIPrep: a robust preprocessing pipeline for functional MRI. Nat. Methods 16, 111–116.
Esterman, M., Noonan, S.K., Rosenberg, M., Degutis, J., 2013. In the zone or zoning out? Tracking behavioral and neural fluctuations during sustained attention. Cereb Cortex 23, 2712–2723.
Esterman, M., Poole, V., Liu, G., DeGutis, J., 2017a. Modulating reward induces differential neurocognitive approaches to sustained attention. Cereb Cortex 27, 4022–4032.
Esterman, M., Reagan, A., Liu, G., Turner, C., DeGutis, J., 2014a. Reward reveals dissociable aspects of sustained attention. J. Exp. Psychol. Gen. 143, 2287–2295.
Esterman, M., Rosenberg, M.D., Noonan, S.K., 2014b. Intrinsic fluctuations in sustained attention and distractor processing. J. Neurosci. 34, 1724–1730.
Esterman, M., Rothlein, D., 2019. Models of sustained attention. Curr. Opin. Psychol. 29, 174–180.
Esterman, M., Thai, M., Okabe, H., DeGutis, J., Saad, E., Laganiere, S.E., Halko, M.A., 2017b. Network-targeted cerebellar transcranial magnetic stimulation improves attentional control. Neuroimage 156, 190–198.
Ezaki, T., Himeno, Y., Watanabe, T., Masuda, N., 2020. Modeling state-transition dynamics in brain signals by memoryless Gaussian mixtures arXiv preprint arXiv:2001.08369.
Ezaki, T., Sakaki, M., Watanabe, T., Masuda, N., 2018. Age-related changes in the ease of dynamical transitions in human brain activity. Hum. Brain Mapp 39, 2673–2688.
Ezaki, T., Watanabe, T., Ohzeki, M., Masuda, N., 2017. Energy landscape analysis of neuroimaging data. Philos. Trans. A Math. Phys. Eng. Sci. 375.
Fiebelkorn, I.C., Kastner, S., 2019. A Rhythmic Theory of Attention. Trends Cogn. Sci. 23, 87–101.
Fiebelkorn, I.C., Pinsk, M.A., Kastner, S., 2018. A dynamic interplay within the frontoparietal network underlies rhythmic spatial attention. Neuron 99, 842–853 e848.
Fong, A.H.C., Yoo, K., Rosenberg, M.D., Zhang, S., Li, C.R., Scheinost, D., Constable, R.T., Chun, M.M., 2019. Dynamic functional connectivity during task performance and rest predicts individual differences in attention across studies. Neuroimage 188, 14–25.
Fortenbaugh, F.C., Corbo, V., Poole, V., McGlinchey, R., Milberg, W., Salat, D., DeGutis, J., Esterman, M., 2017a. Interpersonal early-life trauma alters amygdala connectivity and sustained attention performance. Brain Behav. 7, e00684.
Fortenbaugh, F.C., DeGutis, J., Esterman, M., 2017b. Recent theoretical, neural, and clinical advances in sustained attention research. Ann. N Y Acad. Sci. 1396, 70–91.
Fortenbaugh, F.C., DeGutis, J., Germine, L., Wilmer, J.B., Grosso, M., Russo, K., Esterman, M., 2015. Sustained attention across the life span in a sample of 10,000: dissociating ability and strategy. Psychol. Sci. 26, 1497–1510.
Fortenbaugh, F.C., Rothlein, D., McGlinchey, R., DeGutis, J., Esterman, M., 2018. Tracking behavioral and neural fluctuations during sustained attention: a robust replication and extension. Neuroimage 171, 148–164.
Fox, K.C., Spreng, R.N., Ellamil, M., Andrews-Hanna, J.R., Christoff, K., 2015. The wandering brain: meta-analysis of functional neuroimaging studies of mind-wandering and related spontaneous thought processes. Neuroimage 111, 611–621.
Friston, K., Breakspear, M., Deco, G., 2012. Perception and self-organized instability. Front. Comput. Neurosci. 6, 44.
Gratton, C., Sun, H., Petersen, S.E., 2018. Control networks and hubs. Psychophysiology 55.
Hauser, T.U., Fiore, V.G., Moutoussis, M., Dolan, R.J., 2016. Computational psychiatry of ADHD: neural gain impairments across marrian levels of analysis. Trends Neurosci. 39, 63–73.
Hedges, L.V., 1981. Distribution theory for Glass's estimator of effect size and related estimators. J. Education. Stat. 6, 107–128.
Helfrich, R.F., Fiebelkorn, I.C., Szczepanski, S.M., Lin, J.J., Parvizi, J., Knight, R.T., Kastner, S., 2018. Neural mechanisms of sustained attention are rhythmic. Neuron 99, 854–865 e855.
Hilti, C.C., Jann, K., Heinemann, D., Federspiel, A., Dierks, T., Seifritz, E., Cattapan-Ludewig, K., 2013. Evidence for a cognitive control network for goal-directed attention in simple sustained attention. Brain Cogn. 81, 193–202.
Hinds, O., Thompson, T.W., Ghosh, S., Yoo, J.J., Whitfield-Gabrieli, S., Triantafyllou, C., Gabrieli, J.D., 2013. Roles of default-mode network and supplementary motor area in human vigilance performance: evidence from real-time fMRI. J. Neurophysiol. 109, 1250–1258.
Huang-Pollock, C.L., Karalunas, S.L., Tam, H., Moore, A.N., 2012. Evaluating vigilance deficits in ADHD: a meta-analysis of CPT performance. J. Abnorm Psychol. 121, 360–371.
Jaynes, E.T., 1957. Information theory and statistical mechanics. Phys. Rev. 106, 620–630.
Kelly, A.M., Uddin, L.Q., Biswal, B.B., Castellanos, F.X., Milham, M.P., 2008. Competition between functional brain networks mediates behavioral variability. Neuroimage 39, 527–537.
Kessler, D., Angstadt, M., Sripada, C., 2016. Growth charting of brain connectivity networks and the identification of attention impairment in youth. JAMA Psychiatry 73, 481–489.
Kucyi, A., Daitch, A., Raccah, O., Zhao, B., Zhang, C., Esterman, M., Zeineh, M., Halpern, C.H., Zhang, K., Zhang, J., Parvizi, J., 2020. Electrophysiological dynam-

ics of antagonistic brain networks reflect attentional fluctuations. Nat. Commun. 11, 325.
Kucyi, A., Esterman, M., Riley, C.S., Valera, E.M., 2016. Spontaneous default network activity reflects behavioral variability independent of mind-wandering. Proc. Natl. Acad. Sci. U S A 113, 13899–13904.
Kucyi, A., Hove, M.J., Esterman, M., Hutchison, R.M., Valera, E.M., 2017. Dynamic brain network correlates of spontaneous fluctuations in attention. Cereb. Cortex 27, 1831–1840.
Laird, A.R., Fox, P.M., Eickhoff, S.B., Turner, J.A., Ray, K.L., McKay, D.R., Glahn, D.C., Beckmann, C.F., Smith, S.M., Fox, P.T., 2011. Behavioral interpretations of intrinsic connectivity networks. J. Cogn. Neurosci. 23, 4022–4037.
Langner, R., Eickhoff, S.B., 2013. Sustaining attention to simple tasks: a meta-analytic review of the neural mechanisms of vigilant attention. Psychol. Bull. 139, 870–900.
Lawrence, N.S., Ross, T.J., Hoffmann, R., Garavan, H., Stein, E.A., 2003. Multiple neuronal networks mediate sustained attention. J. Cogn. Neurosci. 15, 1028–1038.
Lorah, J., 2018. Effect size measures for multilevel models: definition, interpretation, and TIMSS example. Large-scale Assess. Education 6.
MacDonald, S.W., Li, S.-C., Bäckman, L., 2009. Neural underpinnings of within-person variability in cognitive functioning. Psychol. Aging 24, 792.
MacDonald, S.W., Nyberg, L., Backman, L., 2006. Intra-individual variability in behavior: links to brain structure, neurotransmission and neuronal activity. Trends Neurosci. 29, 474–480.
Mackworth, N.H., 1948. The breakdown of vigilance during prolonged visual search. Q. J. Exp. Psychol. 1, 6–21.
Marchetta, N.D., Hurks, P.P., De Sonneville, L.M., Krabbendam, L., Jolles, J., 2008. Sustained and focused attention deficits in adult ADHD. J. Atten. Disord. 11, 664–676.
Mason, M.F., Norton, M.I., Van Horn, J.D., Wegner, D.M., Grafton, S.T., Macrae, C.N., 2007. Wandering minds: the default network and stimulus-independent thought. Science 315, 393–395.
Mesmoudi, S., Perlbarg, V., Rudrauf, D., Messe, A., Pinsard, B., Hasboun, D., Cioli, C., Marrelec, G., Toro, R., Benali, H., Burnod, Y., 2013. Resting state networks' corticotopy: the dual intertwined rings architecture. PLoS One 8, e67444.
Mill, R.D., Ito, T., Cole, M.W., 2017. From connectome to cognition: The search for mechanism in human functional brain networks. Neuroimage 160, 124–139.
Mittner, M., Hawkins, G.E., Boekel, W., Forstmann, B.U., 2016. A Neural Model of Mind Wandering. Trends Cogn. Sci. 20, 570–578.
Power, J.D., Cohen, A.L., Nelson, S.M., Wig, G.S., Barnes, K.A., Church, J.A., Vogel, A.C., Laumann, T.O., Miezin, F.M., Schlaggar, B.L., Petersen, S.E., 2011. Functional network organization of the human brain. Neuron 72, 665–678.
Reteig, L.C., van den Brink, R.L., Prinssen, S., Cohen, M.X., Slagter, H.A., 2019. Sustaining attention for a prolonged period of time increases temporal variability in cortical responses. Cortex 117, 16–32.
Rosenberg, M., Noonan, S., DeGutis, J., Esterman, M., 2013. Sustaining visual attention in the face of distraction: a novel gradual-onset continuous performance task. Atten Percept Psychophys. 75, 426–439.
Rosenberg, M.D., Finn, E.S., Scheinost, D., Constable, R.T., Chun, M.M., 2017. Characterizing attention with predictive network models. Trends Cogn. Sci. 21, 290–302.
Rosenberg, M.D., Finn, E.S., Scheinost, D., Papademetris, X., Shen, X., Constable, R.T., Chun, M.M., 2016a. A neuromarker of sustained attention from whole-brain functional connectivity. Nat. Neurosci. 19, 165–171.
Rosenberg, M.D., Scheinost, D., Greene, A.S., Avery, E.W., Kwon, Y.H., Finn, E.S., Ramani, R., Qiu, M., Constable, R.T., Chun, M.M., 2020. Functional connectivity predicts changes in attention observed across minutes, days, and months. Proc. Natl. Acad. Sci. U S A 117, 3797–3807.
Rosenberg, M.D., Zhang, S., Hsu, W.T., Scheinost, D., Finn, E.S., Shen, X., Constable, R.T., Li, C.S., Chun, M.M., 2016b. Methylphenidate Modulates Functional Network Connectivity to Enhance Attention. J. Neurosci. 36, 9547–9557.
Rothlein, D., DeGutis, J., Esterman, M., 2018. Attentional fluctuations influence the neural fidelity and connectivity of stimulus representations. J. Cogn. Neurosci 30, 1209–1228.
Schaefer, A., Kong, R., Gordon, E.M., Laumann, T.O., Zuo, X.N., Holmes, A.J., Eickhoff, S.B., Yeo, B.T.T., 2018. Local-global parcellation of the human cerebral cortex from intrinsic functional connectivity MRI. Cereb Cortex 28, 3095–3114.
Spreng, R.N., Sepulcre, J., Turner, G.R., Stevens, W.D., Schacter, D.L., 2013. Intrinsic architecture underlying the relations among the default, dorsal attention, and frontoparietal control networks of the human brain. J. Cogn. Neurosci. 25, 74–86.
Stawarczyk, D., D'Argembeau, A., 2015. Neural correlates of personal goal processing during episodic future thinking and mind-wandering: an ALE meta-analysis. Hum Brain Mapp. 36, 2928–2947.
Taghia, J., Cai, W., Ryali, S., Kochalka, J., Nicholas, J., Chen, T., Menon, V., 2018. Uncovering hidden brain state dynamics that regulate performance and decision-making during cognition. Nat. Commun. 9, 2505.
Thompson, G.J., Magnuson, M.E., Merritt, M.D., Schwarb, H., Pan, W.J., McKinley, A., Tripp, L.D., Schumacher, E.H., Keilholz, S.D., 2013. Short-time windows of correlation between large-scale functional brain networks predict vigilance intraindividually and interindividually. Hum Brain Mapp. 34, 3280–3298.
Vatansever, D., Menon, D.K., Stamatakis, E.A., 2017. Default mode contributions to automated information processing. Proc. Natl. Acad. Sci. U S A 114, 12821–12826.
Virtanen, P., Gommers, R., Oliphant, T.E., Haberland, M., Reddy, T., Cournapeau, D., Burovski, E., Peterson, P., Weckesser, W., Bright, J., 2019. SciPy 1.0–Fundamental Algorithms for Scientific Computing in Python arXiv preprint arXiv:1907.10121.
Watanabe, T., Hirose, S., Wada, H., Imai, Y., Machida, T., Shirouzu, I., Konishi, S., Miyashita, Y., Masuda, N., 2013. A pairwise maximum entropy model accurately describes resting-state human brain networks. Nat. Commun. 4, 1370.
Watanabe, T., Hirose, S., Wada, H., Imai, Y., Machida, T., Shirouzu, I., Konishi, S., Miyashita, Y., Masuda, N., 2014a. Energy landscapes of resting-state brain networks. Front. Neuroinform 8, 12.
Watanabe, T., Masuda, N., Megumi, F., Kanai, R., Rees, G., 2014b. Energy landscape and dynamics of brain activity during human bistable perception. Nat. Commun. 5, 4765.
Watanabe, T., Rees, G., 2017. Brain network dynamics in high-functioning individuals with autism. Nat. Commun. 8, 16048.
Weissman, D.H., Roberts, K.C., Visscher, K.M., Woldorff, M.G., 2006. The neural bases of momentary lapses in attention. Nat. Neurosci. 9, 971–978.
Yamashita, A., Hayasaka, S., Kawato, M., Imamizu, H., 2017. Connectivity neurofeedback training can differentially change functional connectivity and cognitive performance. Cereb Cortex 27, 4960–4970.